



## Research paper

## Conformational transition of DNA by dinuclear Pt(II) complexes causes cooperative inhibition of gene expression

Yuta Shimizu<sup>a</sup>, Yuko Yoshikawa<sup>a</sup>, Takahiro Kenmotsu<sup>a</sup>, Seiji Komeda<sup>b,\*</sup>, Kenichi Yoshikawa<sup>a,\*</sup><sup>a</sup> Faculty of Life and Medical Sciences, Doshisha University, Kyotanabe 610-0321, Japan<sup>b</sup> Faculty of Pharmaceutical Sciences, Suzuka University of Medical Science, Suzuka 513-8670, Japan

## ARTICLE INFO

## Article history:

Received 8 March 2017

In final form 11 April 2017

Available online 13 April 2017

## Keywords:

Higher-order structure of DNA

Single DNA observation

Anticancer drug

Cooperativity

## ABSTRACT

Recently, it was reported that a cationic tetrazolato-bridged dinuclear Pt(II) complex, 5-H-Y, is a promising anticancer drug candidate. Here, we investigated the effects of a series of tetrazolato-bridged dinuclear Pt(II) complexes on the higher-order structure of DNA by using fluorescence and atomic force microscopies. The results showed that these dinuclear Pt(II) complexes cause marked shrinkage on the conformation of genomic DNA. We also found highly cooperative inhibitory effects of these drugs on *in vitro* gene expression. The unique mechanism of action of these dinuclear Pt(II) complexes is discussed in terms of their bridging effect on DNA segments.

© 2017 The Author(s). Published by Elsevier B.V. This is an open access article under the CC BY-NC-ND license (<http://creativecommons.org/licenses/by-nc-nd/4.0/>).

## 1. Introduction

The effects of various cationic compounds on the structure of DNA have recently attracted considerable attention not only from a physico-chemical point of view but also from researchers in the biological and medical sciences. It has been shown that the addition of multivalent metal cations such as Fe<sup>3+</sup> and [Co(NH<sub>3</sub>)<sub>6</sub>]<sup>3+</sup> induces a large discrete transition in the higher-order structure of genome-sized DNA molecules [1–3]. The clinical significance of metal-DNA interactions was first demonstrated with a mononuclear Pt(II) complex, *cis*-diamminedichloridoplatinum(II) (*cis*-platin) [4], which has become one of the most potent anticancer agents in practical medicine. It has been revealed that Pt-based anticancer agents form covalent Pt–DNA adducts [5,6], such as 1,2-intrastrand crosslinks [7,8] and interstrand crosslinks [9,10]. These physico-chemical studies have led to a basic understanding of the mechanism by which Pt-based anticancer drugs exert their anticancer effects. The particularly high therapeutic efficacy of Pt-based anticancer drugs compared with other anticancer agents inspired studies toward the development of novel Pt-based anti-

cancer drugs [11,12]. It is becoming increasingly clear that cationic dinuclear Pt(II) complexes are potent next generation anticancer drug candidates [13–17]. It has been reported that the tetrazolato-bridged dinuclear Pt(II) complex  $[\{cis\text{-Pt}(\text{NH}_3)_2\}_2(\mu\text{-OH})(\mu\text{-tetrazolato-N2,N3})]^{2+}$  (5-H-Y) exhibit remarkably high antitumor activity in a xenograft nude mouse model of pancreatic cancer [18]. Substitution of two nucleobases for the hydroxo group bridging the two Pt ions, in addition to electrostatic attraction between phosphate groups in DNA and the Pt complex, is considered to provide covalent DNA adducts. Therefore, marked conformational changes in bound DNA, such as shrinkage of DNA chain, are expected to be generated [19–22]. The multimodal DNA binding profile suggests that these dinuclear Pt(II) complexes have a unique mechanism of action to find novel therapeutic applications especially in the treatment of cancers that are insensitive to current Pt-based anticancer drugs.

The cytotoxic effects of cationic di- and tri-nuclear Pt complexes are regarded as closely related to their effects on the higher-order structure of DNA [19,23,24]. Thus, it would be interesting to gain deeper insight into the effects of anti-cancer Pt complexes on the higher-order structure of DNA. In the present study, we investigated effects of a series of highly cytotoxic tetrazolato-bridged dinuclear Pt(II) complexes  $[\{cis\text{-Pt}(\text{NH}_3)_2\}_2(\mu\text{-OH})(\mu\text{-5-R-tetrazolato-N2,N3})](\text{NO}_3)_2$ , where R = CH<sub>2</sub>OCO(CH<sub>2</sub>)<sub>n</sub>CH<sub>3</sub> (*n* = 0 (**1**), 1 (**2**) or 2 (**3**)), as shown in Fig. 1, on the higher-order structure of DNA together with their inhibitory effects on gene expression.

\* Corresponding authors at: Faculty of Pharmaceutical Sciences, Suzuka University of Medical Science, Suzuka, Mie 513-8670, Japan (S. Komeda). Faculty of Life and Medical Sciences, Doshisha University, Kyotanabe, Kyoto 610-0321, Japan (K. Yoshikawa).

E-mail addresses: [komedas@suzuka-u.ac.jp](mailto:komedas@suzuka-u.ac.jp) (S. Komeda), [keyoshik@mail.doshisha.ac.jp](mailto:keyoshik@mail.doshisha.ac.jp) (K. Yoshikawa).

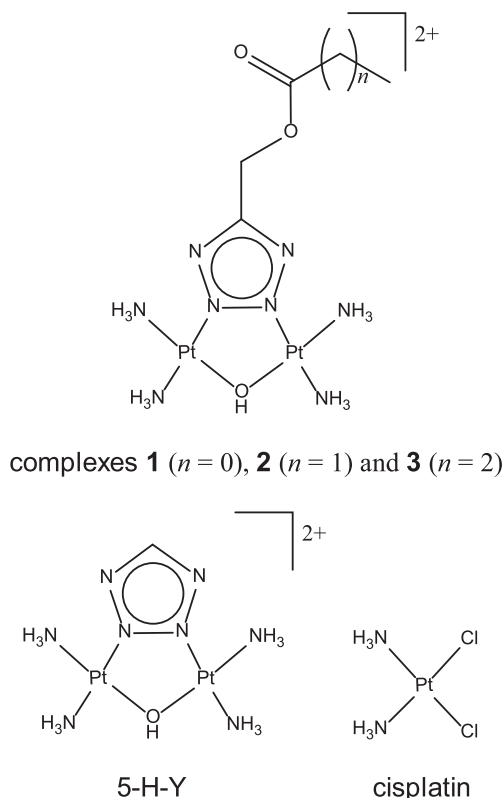


Fig. 1. Chemical structures of Pt(II) complexes used in this study.

## 2. Materials and methods

### 2.1. Materials

T4. GT7 phage DNA (166 kbp, contour length 57  $\mu\text{m}$ ) was purchased from Nippon Gene (Toyama, Japan). The fluorescent cyanine dye YOYO-1 (1,1'-(4,4,7,7-tetramethyl-4,7-diazaundecamethylene)-bis-4-(3-methyl-2,3-dihydro-(benzo-1,3-oxazole)-2-methylidene)-quinolinium tetraiodide) was purchased from Molecular Probes Inc. (Eugene, OR). The antioxidant 2-mercaptoethanol (2-ME) was purchased from Wako Pure Chemical Industries (Osaka, Japan). Tetrazolato-bridged dinuclear Pt(II) complexes were synthesized according to a similar procedure to that described in the literature [25]. Cisplatin was synthesized according to a previous report [26]. Other chemicals were of analytical grade and were obtained from various commercial sources.

### 2.2. Fluorescence microscopy (FM) observation

T4 phage DNA was dissolved in a 10 mM Tris-HCl buffer and 4% (v/v) 2-ME at pH 7.5 in the presence of various concentrations of 5-H-Y, complexes **1–3**, and cisplatin. Measurements were conducted at a low DNA concentration (0.1  $\mu\text{M}$  in nucleotide units). To visualize individual DNA molecules by fluorescence microscopy, 0.05  $\mu\text{M}$  of YOYO-1 was added to the DNA solution after incubation with the complexes. Fluorescent DNA images were obtained using a microscope (Axiovert 135 TV; Carl Zeiss, Oberkochen, Germany) equipped with a 100 $\times$  oil-immersion objective lens and fluorescent illumination from a mercury lamp (100 W) via a filter set (Zeiss-10, excitation BP 450–490; beam splitter FT 510; emission BP 515–565) and with a highly sensitive EBCCD camera (Hamamatsu Photonics, Shizuoka, Japan), which made it possible to record images on DVD at 30 frames per second. The video images were analyzed with Cosmos image-analysis software (Library, Tokyo, Japan).

### 2.3. Atomic Force Microscopy (AFM) observation

For AFM imaging with an SPM-9700 (Shimadzu, Kyoto, Japan), 0.1  $\mu\text{M}$  T4 DNA was dissolved in 10 mM Tris-HCl buffer solution at pH 7.5 with various concentrations of each complex. The DNA solution was incubated for 15 min at room temperature (24  $^{\circ}\text{C}$ ) and then transferred onto a freshly cleaved mica surface. The mica was rinsed with water and dried under nitrogen gas. All imaging was performed in air using the tapping mode. The cantilever, OMCL-AC200TS-C3 (Olympus, Tokyo, Japan), was 200  $\mu\text{m}$  long with a spring constant of 9–20 N/m. The scanning rate was 0.4 Hz and images were captured using the height mode in a 512  $\times$  512 pixel format. The obtained images were plane-fitted and flattened by the computer program supplied with the imaging module before analysis.

### 2.4. Gene expression by Luciferase assay

Cell-free luciferase assays were performed with a TNT T7 Quick Coupled Transcription/Translation System (Promega Co., USA) according to the manufacturer's instructions. Luciferase T7 control DNA (4331 bp) containing a T7 RNA polymerase promoter sequence was used. The DNA concentration was 0.3  $\mu\text{M}$  in nucleotide units. The reaction mixture was incubated for 90 min at 30  $^{\circ}\text{C}$  on a Dry Thermo Unit (TAITEC, Saitama, Japan). Luciferase expression was evaluated following the addition of luciferase substrate (Luciferase Assay Reagent, Promega Co., USA) using a luminometer (MICROTEC Co., Chiba, Japan).

## 3. Results and discussion

### 3.1. Shrinkage of DNA induced by dinuclear Pt(II) complexes

To investigate the effects of dinuclear Pt(II) complexes on the higher-order structure of DNA, we performed FM observations of single DNA molecules in the presence and absence of Pt(II) complexes. Fig. 2 exemplifies the FM images and corresponding quasi-3D profiles of fluorescence intensity in the presence of complex **3**. The time-dependent changes in the pictures indicate that FM enables the observation of individual DNA molecules exhibiting translational and intramolecular Brownian motion in bulk solution. To avoid multi-molecular aggregation, observations were performed at a low DNA concentration (0.1  $\mu\text{M}$ ). In the absence of complex **3**, DNA molecules exist in an elongated coil state (Fig. 2a). Upon the addition of complex **3**, a partial globule conformation is generated as shown in Fig. 2b. With a further increase in complex **3**, DNA molecules exhibit a compact globule conformation (Fig. 2c). These observations clearly indicate that complex **3** markedly affects the higher-order structure by causing a shrunken state.

Fig. 3 shows histograms of the long-axis length  $L$  of DNA as a function of the concentration of Pt(II) complexes together with an assignment of the conformational characteristics in FM images. All of the dinuclear Pt(II) complexes cause shrinkage of the DNA conformation with increase of their concentrations. In contrast, cisplatin has only a very slight effect on the higher-order structure of DNA, as shown in the right-most histogram. The potency for inducing DNA shrinkage is in the order 5-H-Y > complex **3** > complex **2** > complex **1**  $\gg$  cisplatin.

### 3.2. Formation of kinks and bridges

Fig. 4 shows typical AFM images of T4 DNA in the presence of complex **1**, 5-H-Y and cisplatin. With 1.5  $\mu\text{M}$  of 5-H-Y as in Fig. 4a, the overall image contains several micro-kinks as indicated by arrows together with micro-loops. Further additions of 5-H-Y

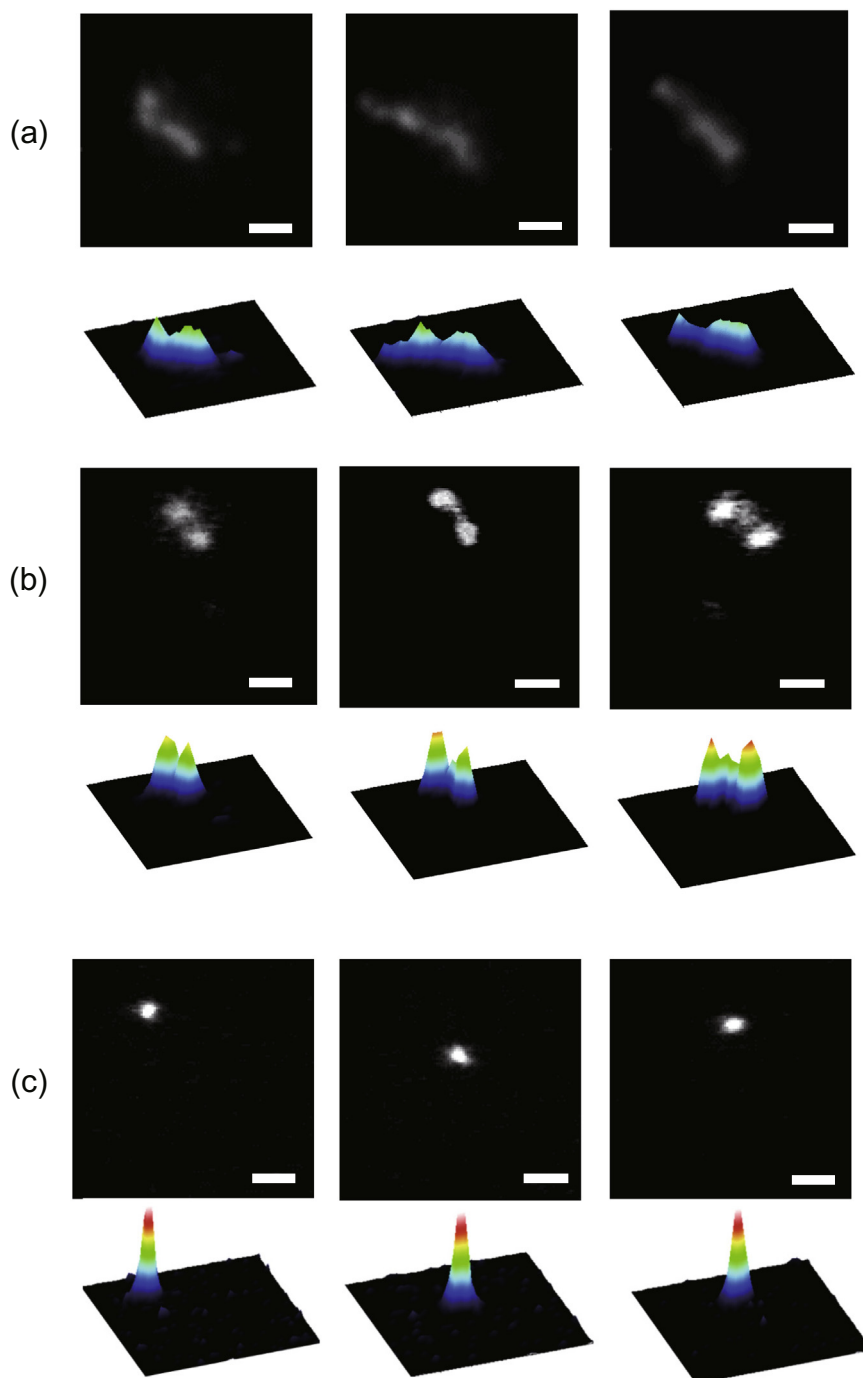


**Fig. 2.** Fluorescence microscopy (FM) observation of single T4 DNA molecules fluctuating in solution under different concentrations of complex **3** and corresponding quasi-3D profiles of the fluorescence intensity: (a) 0  $\mu\text{M}$ , (b) 70  $\mu\text{M}$ , (c) 80  $\mu\text{M}$ . The DNA concentration is 0.1  $\mu\text{M}$  in nucleotide units. The time interval is 0.1 s and the scale bar is 1  $\mu\text{m}$ .

(2.5  $\mu\text{M}$ ) promoted intramolecular bridging among segments, resulting in formation of a partial globule structure (Fig. 4b). Similar to 5-H-Y, 2.5  $\mu\text{M}$  complex **1** generated a loop structure by forming crosslinks (Fig. 4c). In contrast, cisplatin caused kinks/bridges only above 50  $\mu\text{M}$  (Fig. 4d). It has also been reported that DNA shrinkages induced by a series of tetrazolato-bridged dinuclear Pt(II) complexes were characterized as irregular loose packing [23,27–30]. Hou et al. [27] reported their observation that the number of kinks increased gradually during incubation with 77  $\mu\text{M}$  cisplatin for the time scale of several hours through the measurement with AFM on  $\lambda$  DNA.

Based on the observation of the DNA folding transition by FM and AFM, in Fig. 5 we offer a schematic representation of a plausible scenario for the structural change of DNA induced by the dinuclear Pt(II) complexes. At low concentrations of a dinuclear Pt(II) complex, monofunctional binding to the duplex occurs to form diadducts, such as intrastrand crosslinks, or to remain monoadducts which eventually form different diadducts, such as interhelical crosslink, after isomerization reaction in which a Pt(II) ion initially bound to N2 (or N3) of the tetrazole ring migrate to N1 (or N4) [23]. With an increase in the concentration of dinuclear Pt(II) complex, the number of bridges between DNA segments increases

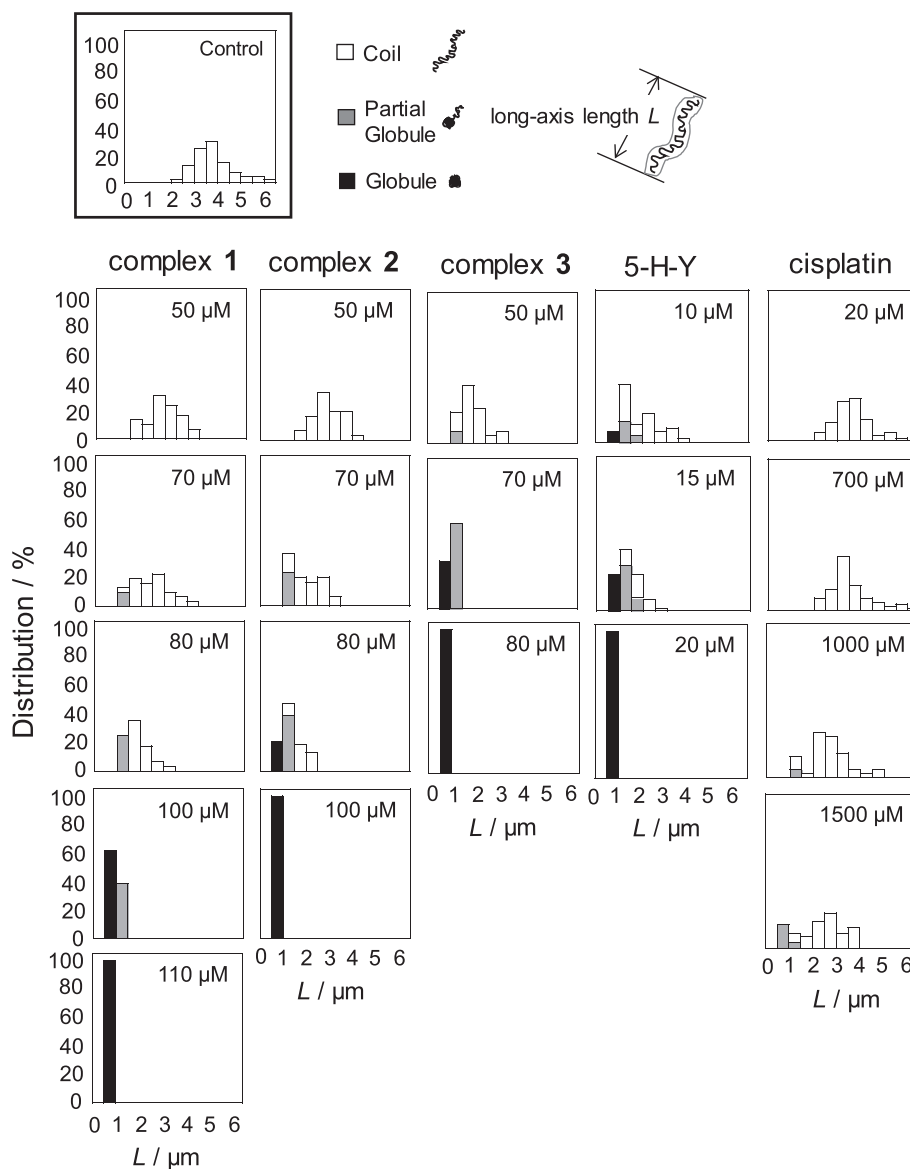


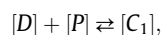
**Fig. 3.** Comparison of the distribution of long-axis length  $L$  of T4 DNA together with an assignment for the conformational characteristics in FM images. The DNA concentration is  $0.1 \mu\text{M}$  in nucleotide units. 70–80 DNA molecules were analyzed at each experimental point.

through the bifunctional DNA binding. The increase in the number of bridges or interhelical crosslinks causes micro-kinks/micro-loops, and, successively, partial globule structure on the DNA chain.

### 3.3. Effect of adducts on luciferase gene expression

To investigate the relationship between the higher-order structure of DNA and gene activity, we carried out a luciferase assay. Fig. 6 shows the dependence of luminescence intensity,  $I_L$ , on the concentration of Pt(II) complex,  $P$ , where the luminescence is generated from luciferase proteins produced through *in vitro* gene expression. In the figure, the luminescence intensity  $I_L$  in the absence of Pt(II) complexes is taken as unity. As shown, the potency for suppressing gene expression is in the order 5-H-Y > complex 3 > complex 2 > complex 1 > cisplatin, corresponding well to the shrinking effect by these Pt(II) complexes. The inhibitory effect is likely attributable to the formation of DNA adducts with the Pt(II) complexes, such as interhelical crosslink, which is a sterically unfavorable binding mode for cisplatin. Thus, we

consider the characteristic effect the process of adduct formation depending on the concentration of Pt(II) complexes. As in the usual expression of ligand binding, the binding equilibrium between DNA binding sites,  $[D]$ , which is defined as the number of binding sites per unit volume, and the concentration of the Pt(II) complex,  $[P]$ , is given as:



where  $[C_1]$  is the concentration of the monoadduct (see Fig. 5).

The equilibrium constant  $K_1$  is given by Eq. (1):

$$K_1 = \frac{[C_1]}{[D][P]}. \quad (1)$$

Then, we consider the binding equilibrium in the formation of the diadduct. Based on the above results with AFM and FM, the DNA molecule shrinks with an increase in the diadduct, i.e., the formation of the diadduct should be highly dependent on the degree of DNA shrinkage. We, thus, propose a scheme on a cooperative

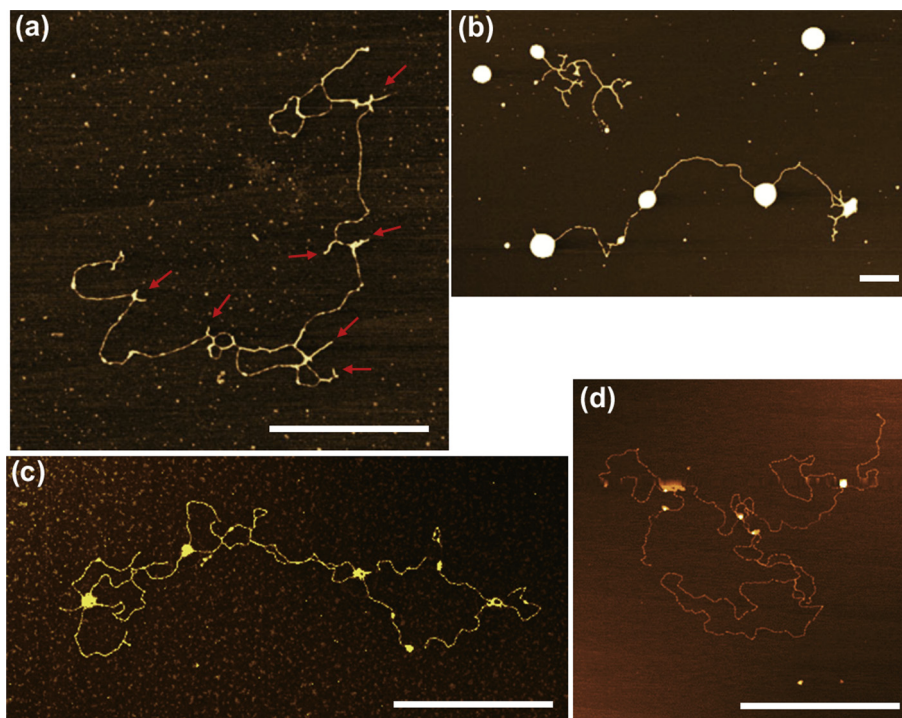


**Fig. 4.** AFM images of T4 DNA in the presence of 5-H-Y, complex 1 and cisplatin under dry condition: (a) 1.5 μM 5-H-Y, (b) 2.5 μM 5-H-Y, (c) 2.5 μM complex 1, (d) 53.3 μM cisplatin. All specimens were gently adsorbed on the mica surface without shear stress. Red arrows in (a) indicate the locations of micro-kinks. The DNA concentration is 0.1 μM in nucleotide units and the scale bar is 1 μm.

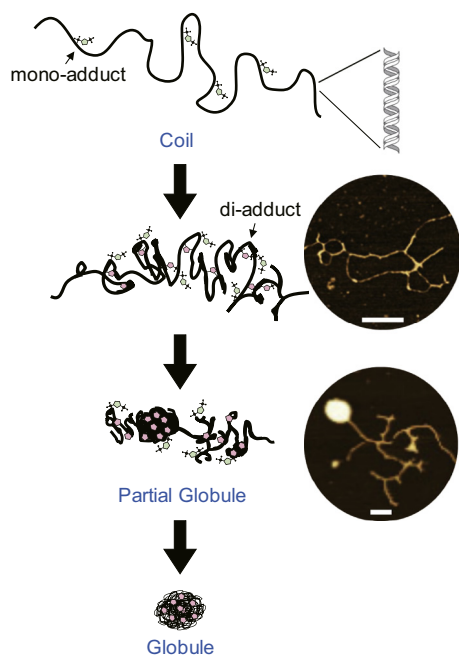


**Fig. 5.** Likely mechanism of DNA shrinking by dinuclear Pt(II) complexes. Mono and diadducts are formed. DNA forms a bridging structure around adducts. DNA is folded into a globule via a partial globule state. Scale bar is 0.5 μm.

increase in the diadduct with an increase in the monoadduct. By introducing a parameter of cooperativity on the diadduct formation as  $m$ , we obtain the binding equilibrium as:

$$[C_1] + m[P] \rightleftharpoons [C_2].$$

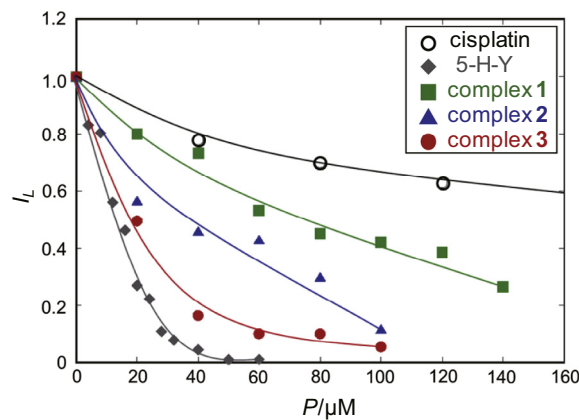


**Fig. 6.** Relative luminescence intensity ( $I_L$ ) vs. concentrations of Pt(III) complexes ( $P$ ). The activity in each graph is normalized to that in the absence of Pt(II) complexes. The fitting lines are drawn to guide the eye.

where  $[C_2]$  is the concentration of DNA domain bound with plural number of diadduct as a result of cooperative binding of the Pt(II) complex.

The equilibrium constant  $K_2$  is given as

$$K_2 = \frac{[C_2]}{[C_1][P]^m}. \quad (2)$$

The total concentration of DNA binding sites,  $D_0$  is the sum of the sites of free, monoadduct formation, as in Eq. (3):

$$D + C_1 + C_2 \approx D_0. \quad (3)$$

From Eqs. (1)–(3), we derive Eq. (4):

$$\frac{D_0}{D} - 1 \approx K_1P + K_1K_2P^m. \quad (4)$$

In the following analysis of the experimental data, we take the parameter of cooperativity to be  $m = 3$ , for simplicity.

Now, we may regard that the relative luminescence intensity  $I_L$  in Fig. 6 corresponds to the portion of DNA site without the inhibitory effect of Pt-binding. That is,  $I_L \approx \frac{D_0}{D_0 + P}$ , and Eq. (4) becomes as follows:

$$\frac{1}{I_L} - 1 \approx K_1 P + K_1 K_2 P^3. \quad (5)$$

Fig. 7 shows the dependence of  $\frac{1}{I_L} - 1$  on the concentration,  $P$ , of added Pt(II) complexes, based on the experimental data given in Fig. 6. By using the relationship in Eq. (5), we analyzed the experimental curves in Fig. 7. The inset in Fig. 7 shows the near-linear relationship between  $\frac{1}{I_L} - 1$  and  $P$ , indicating that the binding equilibrium at low concentrations of the Pt(II) complexes reflects the formation of the monoadduct. Thus, from the linear regime, we can evaluate the equilibrium constant  $K_1$  for the formation of the monoadduct. From curve-fitting with Eq. (5), we can deduce the equilibrium constant  $K_2$ . The apparent binding equilibrium constants,  $K_1$  and  $K_2$ , are summarized in Table 1. It is noted that there is a very large difference in  $K_2$  between the derivatives of 5-H-Y and cisplatin, indicating significance in the cooperative binding of the dinuclear Pt(II) complexes in contrast to the negligible effect with cisplatin. On the other hand, the differences in  $K_1$  between the 5-H-Y derivatives and cisplatin are not so large. Thus, the proposed scheme with the binding equilibria as in Eqs. (1) and (2) will explain the experimental tendency on the change in the higher-order structure of DNA and also on the compound's inhibitory effect on gene expression. As for the binding equilibrium of cisplatin to DNA, Crisafuli et al. estimated the change of persistence length based on their measurement of stretching experiments on single  $\lambda$ -DNA molecules at different cisplatin concentrations [31]. They found a steep decrease of the persistence length above the cisplatin concentration of ca. 70–80  $\mu\text{M}$  and discussed such behavior in terms of a weak cooperative effect of cisplatin binding. It is noted that our observation on the inhibitory effect on gene expression by cisplatin corresponds to the change of the persistence length reported by them [31].

It is of interest that the order of efficiency of the dinuclear Pt(II) complexes for both induction of DNA shrinking and the inhibition of gene expression is 5-H-Y > complex 3 > complex 2 > complex 1, regardless the difference in the detailed experimental conditions

**Table 1**  
Binding affinities,  $K_1$  and  $K_2$ , of Pt(II) complexes.

Complex	$K_1$ [ $\times 10^{-3} \mu\text{M}^{-1}$ ]	$K_2$ [ $\times 10^{-4} \mu\text{M}^{-2}$ ]
Cisplatin	4	<0.1
5-H-Y	22	140
Complex 1	7	1
Complex 2	14	4
Complex 3	20	14

between the structural study with FM and AFM, and the gene expression assay. To understand the above ordering, as the next research it would be valuable to interpret the differences of their activities in terms of chemical interactions, such as electrostatic effect, steric hindrance, and hydrophobic effect.

#### 4. Conclusion

In the present study, we focused on the change in the higher-order structure of DNA induced by tetrazolato-bridged dinuclear Pt(II) complexes, together with their inhibitory effects on gene expression. Our observation revealed that these dinuclear Pt(II) complexes, at concentrations on the order of  $\mu\text{M}$ , cause DNA shrinkage, whereas cisplatin has almost no effect at such a low concentration. In addition, the potency to induce shrinkage is in the order 5-H-Y > complex 3 > complex 2 > complex 1. It was found that these dinuclear Pt(II) complexes cause shrinking of DNA through the formation of kinks and bridges.

The potency for suppression against gene expression is in the order 5-H-Y > complex 3 > complex 2 > complex 1  $\gg$  cisplatin. At low concentrations, simple non-cooperative binding occurs. With the increase of concentration, these dinuclear Pt(II) complexes successively adduct to DNA segments in a cooperative manner and drastically suppress gene expression.

This study revealed a direct relationship between a change in the higher-order structure of DNA and an effect on gene expression [32]. In addition, we obtained results that could serve as a clue to elucidating the unique mechanism of action of tetrazolato-bridged dinuclear Pt(II) complexes, which have potential as next-generation Pt-based anticancer drugs. These evaluations may contribute to the development of new methods for screening drugs.

#### Acknowledgements

This work was partially supported by JSPS KAKENHI Grant Numbers 15H02121, 15K07905 and 25103012. We are grateful to Drs. S. Harusawa and H. Yoneyama at Osaka University of Pharmaceutical Sciences for providing synthetic materials for the dinuclear Pt(II) complexes.

#### References

- [1] J. Wisdom, R.L. Baldwin, Monomolecular condensation of DNA induced by cobalt hexamine, *Biopolymer* 22 (1983) 1595.
- [2] Y. Yamasaki, K. Yoshikawa, Higher order structure of DNA controlled by redox state of  $\text{Fe}^{2+}/\text{Fe}^{3+}$ , *J. Am. Chem. Soc.* 119 (1997) 10573.
- [3] K. Yoshikawa, S. Kidoaki, M. Takahashi, V.V. Vasilevskaya, A.R. Khokhlov, Marked discreteness on the coil-globule transition of single duplex DNA, *Ber. Bunsenges. Phys. Chem.* 100 (1996) 876.
- [4] B. Rosenberg, L. Vancamp, J.E. Trosko, V.H. Mansour, Platinum compounds: a new class of potent antitumour agents, *Nature* 222 (1969) 385.
- [5] A.M. Fichtinger-Schepman, P.H. Lohman, J. Reedijk, Detection and quantification of adducts formed upon interaction of diamminedichloroplatinum (II) with DNA, by anion-exchange chromatography after enzymatic degradation, *Nucleic Acids Res.* 10 (1982) 5345.
- [6] D. Salerno, G.L. Beretta, G. Zanchetta, S. Brioschi, M. Cristofalo, N. Missana, L. Nardo, V. Cassina, A. Tempestini, R. Giovannoni, M.G. Cerrito, N. Zaffaroni, T. Bellini, F. Mantegazza, Platinum-based drugs and DNA interactions studied by single-molecule and bulk measurements, *Biophys. J.* 110 (2016) 2151.

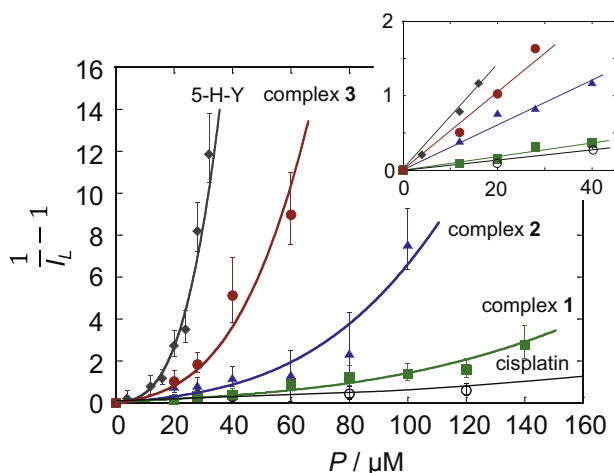


**Fig. 7.** Relationship between  $P$  and  $\frac{1}{I_L} - 1$ , where  $I_L$  corresponds to  $\frac{D_0}{D_0 + P}$ . The activity in each graph is normalized to that in the absence of Pt(II) complexes. Inset is the enlarged view on the graph for low concentrations of Pt(II) complexes. The error bars indicate standard errors.

- [7] P.M. Takahara, A.C. Rosenzweig, C.A. Frederick, S.J. Lippard, Crystal structure of double-stranded DNA containing the major adduct of the anticancer drug cisplatin, *Nature* 377 (1995) 649.
- [8] A. Eastman, Reevaluation of interaction of cis-dichloro (ethylenediamine)platinum(II) with DNA, *Biochemistry* 25 (1986) 3912.
- [9] J.-M. Malinge, M. Leng, Interstrand cross-links in cisplatin- or transplatin-modified DNA, in: B. Lippert (Ed.), *Cisplatin: Chemistry and Biochemistry of a Leading Anticancer Drug*, Verlag Helvetica Chimica Acta, Zürich, 1999, pp. 159–180, Chap. 6.
- [10] F. Coste, J.-M. Malinge, L. Serre, M. Leng, C. Zelwer, W. Shepard, M. Roth, Crystal structure of a double-stranded DNA containing a cisplatin interstrand cross-link at 1.63 Å resolution: hydration at the platinated site, *Nucleic Acids Res.* 27 (1999) 1837.
- [11] S. Dilruba, G.V. Kalayda, Platinum-based drugs: past, present and future, *Cancer Chemother. Pharmacol.* 77 (2016) 1103.
- [12] D.J. Stewart, Mechanisms of resistance to cisplatin and carboplatin, *Crit. Rev. Oncol. Hematol.* 63 (2007) 12.
- [13] N. Farrell, Multi-platinum anti-cancer agents. Substitution-inert compounds for tumor selectivity and new targets, *Chem. Soc. Rev.* 44 (2015) 8773.
- [14] N. Farrell, Polynuclear platinum drugs, *Met. Ions Biol. Syst.* 42 (2004) 251.
- [15] T. Boulikas, A. Pantos, E. Bellis, P. Christofis, Designing platinum compounds in cancer: structures and mechanisms, *Cancer Ther.* 5 (2007) 537.
- [16] S. Komeda, Unique platinum-DNA interactions may lead to more effective platinum-based antitumor drugs, *Metallomics* 3 (2011) 650.
- [17] L. Kelland, The resurgence of platinum-based cancer chemotherapy, *Nat. Rev. Cancer* 7 (2007) 573.
- [18] S. Komeda, Y.-L. Lin, M. Chikuma, A tetrazolato-bridged dinuclear platinum(II) complex exhibits markedly high in vivo antitumor activity against pancreatic cancer, *ChemMedChem* 6 (2011) 987.
- [19] R. Imai, S. Komeda, M. Shimura, S. Tamura, S. Matsuyama, K. Nishimura, R. Rogge, A. Matsunaga, I. Hiratani, H. Takata, M. Uemura, Y. Iida, Y. Yoshikawa, J. C. Hansen, K. Yamauchi, M.T. Kanemaki, K. Maeshima, Chromatin folding and DNA replication inhibition mediated by a highly antitumor-active tetrazolato-bridged dinuclear platinum(II) complex, *Sci. Rep.* 6 (2016) 24712.
- [20] M. Uemura, M. Hoshiyama, A. Furukawa, T. Sato, Y. Higuchi, S. Komeda, Highly efficient uptake into cisplatin-resistant cells and the isomerization upon coordinative DNA binding of anticancer tetrazolato-bridged dinuclear platinum(II) complexes, *Metallomics* 7 (2015) 1488.
- [21] N. Kida, Y. Katsuda, Y. Yoshikawa, S. Komeda, T. Sato, Y. Saito, M. Chikuma, M. Suzuki, T. Imanaka, K. Yoshikawa, Characteristic effect of an anticancer dinuclear platinum(II) complex on the higher-order structure of DNA, *J. Biol. Inorg. Chem.* 15 (2010) 701.
- [22] M. Uemura, Y. Yoshikawa, K. Yoshikawa, T. Sato, Y. Mino, M. Chikuma, S. Komeda, Second- and higher-order structural changes of DNA induced by antitumor-active tetrazolato-bridged dinuclear platinum(II) complexes with different types of 5-substituent, *J. Inorg. Biochem.* 127 (2013) 169.
- [23] J. Malina, N.P. Farrell, V. Brabec, Substitution-inert trinuclear platinum complexes efficiently condense/aggregate nucleic acids and inhibit enzymatic activity, *Angew. Chem. Int. Ed.* 53 (2014) 12812.
- [24] J. Malina, N.P. Farrell, V. Brabec, DNA condensing effects and sequence selectivity of DNA binding of antitumor noncovalent polynuclear platinum complexes, *Inorg. Chem.* 53 (2014) 1662.
- [25] S. Komeda, H. Takayama, T. Suzuki, A. Odani, T. Yamori, M. Chikuma, Synthesis of antitumor azolato-bridged dinuclear platinum(ii) complexes with in vivo antitumor efficacy and unique in vitro cytotoxicity profiles, *Metallomics* 5 (2013) 461.
- [26] R.A. Alderden, T.W. Hambley, The discovery and development of cisplatin, *J. Chem. Educ.* 83 (2006) 728.
- [27] X.M. Hou, X.H. Zhang, K.J. Wei, C. Ji, S.X. Dou, W.C. Wang, M. Li, P.Y. Wang, Cisplatin induces loop structures and condensation of single DNA molecules, *Nucleic Acids Res.* 37 (2009) 1400.
- [28] Y. Yoshikawa, S. Komeda, M. Uemura, T. Kanbe, M. Chikuma, K. Yoshikawa, T. Imanaka, Highly efficient DNA compaction mediated by an in vivo antitumor-active tetrazolato-bridged dinuclear platinum(II) complex, *Inorg. Chem.* 50 (2011) 11729.
- [29] S. Komeda, H. Yoneyama, M. Uemura, A. Muramatsu, N. Okamoto, H. Konishi, H. Takahashi, A. Takagi, W. Fukuda, T. Imanaka, T. Kanbe, S. Harusawa, Y. Yoshikawa, K. Yoshikawa, Specific conformational change in giant DNA caused by anticancer tetrazolato-bridged dinuclear platinum(II) complexes: middle-length alkyl substituents exhibit minimum effect, *Inorg. Chem.* 56 (2017) 802.
- [30] Z. Liu, S. Tan, Y. Zu, Y. Fu, R. Meng, Z. Xing, The interactions of cisplatin and DNA studied by atomic force microscopy, *Micron* 41 (2010) 833.
- [31] F.A.P. Crisafuli, E.C. Cesconetto, E.B. Ramos, M.S. Rocha, DNA-cisplatin binding mechanism peculiarities studied with single molecule stretching experiments, *Appl. Phys. Lett.* 100 (2012) 083701.
- [32] A. Estévez-Torres, D. Baigl, DNA compaction: fundamentals and applications, *Soft Matter* 7 (2011) 6746.